

# A study of $\gamma\gamma \rightarrow K_S^0 K_S^0$ production at energies from 2.4 to 4.0 GeV at Belle

Belle Collaboration

W.T. Chen<sup>v,\*</sup>, K. Abe<sup>h</sup>, K. Abe<sup>ao</sup>, I. Adachi<sup>h</sup>, H. Aihara<sup>aq</sup>, D. Anipko<sup>a</sup>, V. Aulchenko<sup>a</sup>,  
A.M. Bakich<sup>al</sup>, E. Barberio<sup>s</sup>, A. Bay<sup>p</sup>, I. Bedny<sup>a</sup>, U. Bitenc<sup>m</sup>, I. Bizjak<sup>m</sup>, S. Blyth<sup>v</sup>, A. Bondar<sup>a</sup>,  
A. Bozek<sup>y</sup>, M. Bračko<sup>h,r,m</sup>, T.E. Browder<sup>g</sup>, M.-C. Chang<sup>e</sup>, P. Chang<sup>x</sup>, Y. Chao<sup>x</sup>, A. Chen<sup>v</sup>,  
B.G. Cheon<sup>c</sup>, R. Chistov<sup>l</sup>, Y. Choi<sup>ak</sup>, Y.K. Choi<sup>ak</sup>, J. Dalseno<sup>s</sup>, M. Dash<sup>au</sup>, A. Drutskoy<sup>d</sup>,  
S. Eidelman<sup>a</sup>, D. Epifanov<sup>a</sup>, A. Go<sup>v</sup>, H. Ha<sup>o</sup>, M. Hazumi<sup>h</sup>, D. Heffernan<sup>ad</sup>, T. Higuchi<sup>aq</sup>,  
T. Hokuue<sup>t</sup>, Y. Hoshi<sup>ao</sup>, W.-S. Hou<sup>x</sup>, T. Iijima<sup>t</sup>, A. Imoto<sup>u</sup>, K. Inami<sup>t</sup>, A. Ishikawa<sup>aq</sup>, R. Itoh<sup>h</sup>,  
M. Iwasaki<sup>aq</sup>, H. Kaji<sup>t</sup>, J.H. Kang<sup>av</sup>, P. Kapusta<sup>y</sup>, N. Katayama<sup>h</sup>, H. Kawai<sup>b</sup>, T. Kawasaki<sup>aa</sup>,  
H. Kichimi<sup>h</sup>, H.O. Kim<sup>ak</sup>, Y.J. Kim<sup>f</sup>, S. Korpar<sup>r,m</sup>, P. Križan<sup>q,m</sup>, P. Krokovny<sup>h</sup>, R. Kulasiri<sup>d</sup>,  
R. Kumar<sup>ae</sup>, C.C. Kuo<sup>v</sup>, A. Kuzmin<sup>a</sup>, Y.-J. Kwon<sup>av</sup>, S.E. Lee<sup>ai</sup>, T. Lesiak<sup>y</sup>, S.-W. Lin<sup>x</sup>,  
D. Liventsev<sup>l</sup>, G. Majumder<sup>am</sup>, F. Mandl<sup>k</sup>, T. Matsumoto<sup>as</sup>, A. Matyja<sup>y</sup>, S. McOnie<sup>al</sup>,  
T. Medvedeva<sup>l</sup>, H. Miyata<sup>aa</sup>, Y. Miyazaki<sup>t</sup>, R. Mizuk<sup>l</sup>, G.R. Moloney<sup>s</sup>, T. Mori<sup>t</sup>, E. Nakano<sup>ac</sup>,  
M. Nakao<sup>h</sup>, H. Nakazawa<sup>v</sup>, Z. Natkaniec<sup>y</sup>, S. Nishida<sup>h</sup>, O. Nitoh<sup>at</sup>, T. Nozaki<sup>h</sup>, S. Ogawa<sup>an</sup>,  
T. Ohshima<sup>t</sup>, S. Okuno<sup>n</sup>, S.L. Olsen<sup>g</sup>, Y. Onuki<sup>ag</sup>, H. Ozaki<sup>h</sup>, P. Pakhlov<sup>l</sup>, G. Pakhlova<sup>l</sup>, H. Palka<sup>y</sup>,  
C.W. Park<sup>ak</sup>, R. Pestotnik<sup>m</sup>, L.E. Piilonen<sup>au</sup>, H. Sahoo<sup>g</sup>, Y. Sakai<sup>h</sup>, N. Satoyama<sup>aj</sup>, T. Schietinger<sup>p</sup>,  
O. Schneider<sup>p</sup>, J. Schümann<sup>h</sup>, K. Senyo<sup>t</sup>, M.E. Sevior<sup>s</sup>, M. Shapkin<sup>j</sup>, H. Shibuya<sup>an</sup>, B. Shwartz<sup>a</sup>,  
J.B. Singh<sup>ae</sup>, A. Sokolov<sup>j</sup>, A. Somov<sup>d</sup>, N. Soni<sup>ae</sup>, S. Stanič<sup>ab</sup>, M. Starič<sup>m</sup>, H. Stoeck<sup>al</sup>,  
S.Y. Suzuki<sup>h</sup>, F. Takasaki<sup>h</sup>, K. Tamai<sup>h</sup>, M. Tanaka<sup>h</sup>, G.N. Taylor<sup>s</sup>, Y. Teramoto<sup>ac</sup>, X.C. Tian<sup>af</sup>,  
I. Tikhomirov<sup>l</sup>, T. Tsukamoto<sup>h</sup>, S. Uehara<sup>h</sup>, K. Ueno<sup>x</sup>, T. Uglov<sup>l</sup>, Y. Unno<sup>c</sup>, S. Uno<sup>h</sup>, Y. Usov<sup>a</sup>,  
G. Varner<sup>g</sup>, K. Vervink<sup>p</sup>, S. Villa<sup>p</sup>, C.C. Wang<sup>x</sup>, C.H. Wang<sup>w</sup>, M.-Z. Wang<sup>x</sup>, Y. Watanabe<sup>ar</sup>,  
E. Won<sup>o</sup>, B.D. Yabsley<sup>al</sup>, A. Yamaguchi<sup>ap</sup>, Y. Yamashita<sup>z</sup>, M. Yamauchi<sup>h</sup>, C.C. Zhang<sup>i</sup>,  
Z.P. Zhang<sup>ah</sup>, V. Zhilich<sup>a</sup>, A. Zupanc<sup>m</sup>

<sup>a</sup> Budker Institute of Nuclear Physics, Novosibirsk, Russia

<sup>b</sup> Chiba University, Chiba, Japan

<sup>c</sup> Hanyang University, Seoul, South Korea

<sup>d</sup> University of Cincinnati, Cincinnati, OH, USA

<sup>e</sup> Department of Physics, Fu Jen Catholic University, Taipei, Taiwan

<sup>f</sup> The Graduate University for Advanced Studies, Hayama, Japan

<sup>g</sup> University of Hawaii, Honolulu, HI, USA

<sup>h</sup> High Energy Accelerator Research Organization (KEK), Tsukuba, Japan

<sup>i</sup> Institute of High Energy Physics, Chinese Academy of Sciences, Beijing, PR China

<sup>j</sup> Institute for High Energy Physics, Protvino, Russia

<sup>k</sup> Institute of High Energy Physics, Vienna, Austria

<sup>l</sup> Institute for Theoretical and Experimental Physics, Moscow, Russia

<sup>m</sup> J. Stefan Institute, Ljubljana, Slovenia

<sup>n</sup> Kanagawa University, Yokohama, Japan

<sup>o</sup> Korea University, Seoul, South Korea

<sup>p</sup> Swiss Federal Institute of Technology of Lausanne, EPFL, Lausanne, Switzerland

<sup>q</sup> University of Ljubljana, Ljubljana, Slovenia

<sup>r</sup> University of Maribor, Maribor, Slovenia

<sup>s</sup> University of Melbourne, Victoria, Australia

- <sup>†</sup> Nagoya University, Nagoya, Japan  
<sup>u</sup> Nara Women's University, Nara, Japan  
<sup>v</sup> National Central University, Chung-li, Taiwan  
<sup>w</sup> National United University, Miao Li, Taiwan  
<sup>x</sup> Department of Physics, National Taiwan University, Taipei, Taiwan  
<sup>y</sup> H. Niewodniczanski Institute of Nuclear Physics, Krakow, Poland  
<sup>z</sup> Nippon Dental University, Niigata, Japan  
<sup>aa</sup> Niigata University, Niigata, Japan  
<sup>ab</sup> University of Nova Gorica, Nova Gorica, Slovenia  
<sup>ac</sup> Osaka City University, Osaka, Japan  
<sup>ad</sup> Osaka University, Osaka, Japan  
<sup>ae</sup> Panjab University, Chandigarh, India  
<sup>af</sup> Peking University, Beijing, PR China  
<sup>ag</sup> RIKEN BNL Research Center, Brookhaven, NY, USA  
<sup>ah</sup> University of Science and Technology of China, Hefei, PR China  
<sup>ai</sup> Seoul National University, Seoul, South Korea  
<sup>aj</sup> Shinshu University, Nagano, Japan  
<sup>ak</sup> Sungkyunkwan University, Suwon, South Korea  
<sup>al</sup> University of Sydney, Sydney, NSW, Australia  
<sup>am</sup> Tata Institute of Fundamental Research, Bombay, India  
<sup>an</sup> Toho University, Funabashi, Japan  
<sup>ao</sup> Tohoku Gakuin University, Tagajo, Japan  
<sup>ap</sup> Tohoku University, Sendai, Japan  
<sup>aq</sup> Department of Physics, University of Tokyo, Tokyo, Japan  
<sup>ar</sup> Tokyo Institute of Technology, Tokyo, Japan  
<sup>as</sup> Tokyo Metropolitan University, Tokyo, Japan  
<sup>at</sup> Tokyo University of Agriculture and Technology, Tokyo, Japan  
<sup>au</sup> Virginia Polytechnic Institute and State University, Blacksburg, VA, USA  
<sup>av</sup> Yonsei University, Seoul, South Korea

Received 16 April 2007; accepted 22 May 2007

Available online 5 June 2007

Editor: M. Doser

## Abstract

$K_S^0 K_S^0$  production in two-photon collisions has been studied using a  $397.6 \text{ fb}^{-1}$  data sample collected with the Belle detector at the KEKB  $e^+e^-$  collider. For the first time the cross sections are measured in the two-photon center-of-mass energy range between 2.4 GeV and 4.0 GeV and angular range  $|\cos\theta^*| < 0.6$ . Combining the results with measurements of  $\gamma\gamma \rightarrow K^+K^-$  from Belle, we observe that the cross section ratio  $\sigma(K_S^0 K_S^0)/\sigma(K^+K^-)$  decreases from  $\sim 0.13$  to  $\sim 0.01$  with increasing energy. Signals for the  $\chi_{c0}$  and  $\chi_{c2}$  charmonium states are also observed. © 2007 Elsevier B.V. All rights reserved.

PACS: 12.38.Qk; 13.85.Lg; 13.66.Bc; 13.25.Gv

Keywords: Two-photon collisions; Mesons; QCD; Charmonium

## 1. Introduction

Exclusive processes with hadronic final states in two-photon collision are an excellent probe to test various model calculations motivated by perturbative and non-perturbative QCD. As shown by Brodsky and Lepage (BL) [1], at sufficiently large two-photon center-of-mass energy  $\sqrt{s}$  and momentum transfer from the initial photon to the produced meson  $t$ , the leading term of the amplitude for the process  $\gamma\gamma \rightarrow M\bar{M}$ , where  $M$  denotes a meson, can be expressed as a hard scattering amplitude for  $\gamma\gamma \rightarrow q\bar{q}q\bar{q}$  times the leading term meson electromagnetic form factor. For mesons with zero helicity their

calculation gives the following dependence on  $s$  and scattering angle  $\theta^*$ :

$$\frac{d\sigma^{\text{lead}}}{d|\cos\theta^*|} = 16\pi\alpha^2 \frac{|F_M^{\text{lead}}(s)|^2}{s} \times \left\{ \frac{[(e_1 - e_2)^2]^2}{(1 - \cos^2\theta^*)^2} + \frac{2(e_1 e_2)[(e_1 - e_2)^2]}{1 - \cos^2\theta^*} g(\theta^*) + 2(e_1 e_2)^2 g^2(\theta^*) \right\}, \quad (1)$$

where  $e_1$  and  $e_2$  are the quark charges (i.e., mesons have charges  $\pm(e_1 - e_2)$ ), and explicit forms of the leading term meson form factor  $F_M^{\text{lead}}(s)$  ( $F_M^{\text{lead}}(s) \sim 1/s$  at  $s \rightarrow \infty$ ) and the function  $g(\theta^*)$  can be found in Refs. [1,2]. Eq. (1) implies that the angular distribution of neutral meson pairs, unlike that for

\* Corresponding author.

E-mail address: wtchen@hepsrv.phy.ncu.edu.tw (W.T. Chen).

charged meson pairs which is dominated by  $\sim \sin^{-4}\theta^*$  terms, is directly determined by the shape of  $g(\theta^*)$  and the value of  $F_M^{\text{lead}}(s)$ . Later, Benayoun and Chernyak (BC) [2] used a factorization hypothesis similar to the BL calculation but further improved the treatment of the effects of SU(3) symmetry breaking; their predictions appeared to be in good agreement with the subsequent measurements of  $\gamma\gamma \rightarrow \pi^+\pi^-$  and  $\gamma\gamma \rightarrow K^+K^-$  [3,4].

Recently, Diehl, Kroll and Vogt (DKV) [5] considered the consequences of the assumption that at intermediate energies the amplitudes for the process  $\gamma\gamma \rightarrow M\bar{M}$  are dominated by so-called handbag contributions. The handbag amplitude is expressed as the product of an amplitude for the hard  $\gamma\gamma \rightarrow q\bar{q}$  subprocess times an unknown form factor  $R_{M\bar{M}}(s)$  describing the soft transition from the  $q\bar{q}$  to the meson pair. In [5] the differential cross section is given by

$$\frac{d\sigma}{d|\cos\theta^*|}(\gamma\gamma \rightarrow M\bar{M}) = \frac{8\pi\alpha^2}{s} \frac{1}{\sin^4\theta^*} |R_{M\bar{M}}(s)|^2, \quad (2)$$

where the meson annihilation form factor  $R_{M\bar{M}}(s)$  is not calculated in Ref. [5] but is instead obtained by fitting the data; the magnitude of  $R_{M\bar{M}}(s)$  for different mesons can be linked by using SU(3) and isospin symmetry. The validity of this approach has recently been criticized in Ref. [6].

Earlier, the Belle Collaboration performed a high-statistics measurement of the cross sections for the processes  $\gamma\gamma \rightarrow \pi^+\pi^-$  and  $\gamma\gamma \rightarrow K^+K^-$  [4] in the  $W(=\sqrt{s})$  range 2.4 GeV <  $W$  < 4.1 GeV. Analysis of the data showed that in this  $W$  range the  $W$ -dependence of the cross section is consistent with that predicted by the leading term QCD calculations [1,2]. Here we report a measurement of the cross section for  $\gamma\gamma \rightarrow K_S^0 K_S^0$  at 2.4 GeV <  $W$  < 4.0 GeV and  $|\cos\theta^*| < 0.6$  with a data sample of 397.6 fb<sup>-1</sup> collected at or near the  $\Upsilon(4S)$  resonance, accumulated with the Belle detector [7] at the KEKB asymmetric-energy  $e^+e^-$  collider [8]. This measurement can provide important information that complements previous studies and sheds light on how the two-photon mass and angular distributions of such cross sections depend on the flavor of the produced mesons.

The Belle detector is a large-solid-angle magnetic spectrometer. Momenta of charged tracks are measured with a central drift chamber (CDC), located in a uniform 1.5 T magnetic field which surrounds the interaction point (IP) and subtends the polar angle range  $17^\circ < \theta_{\text{lab}} < 150^\circ$ , where  $\theta_{\text{lab}}$  is a scattering angle in the laboratory frame. The trajectories of the charged tracks near the interaction point are provided by the CDC and the silicon vertex detector (SVD). Energy measurement of electromagnetically interacting particles is performed in an electromagnetic calorimeter (ECL) made up of CsI (TI) crystals. The detector is described in detail elsewhere [7].

## 2. Event selection

Exclusive  $K_S^0 K_S^0$  pairs are produced in quasi-real two-photon collisions through the process  $e^+e^- \rightarrow e^+e^-\gamma\gamma \rightarrow$

$e^+e^- K_S^0 K_S^0$ , where the scattered  $e^+$  and  $e^-$  are lost down the beampipe, and only the two  $K_S^0$  mesons are detected.

We select  $\gamma\gamma \rightarrow K_S^0 K_S^0$  candidate events in two stages. At stage I the following requirements are applied:

- exactly four charged tracks with zero net charge of which at least two have  $p_t > 0.3$  GeV/c,  $dr < 1$  cm,  $|dz| < 5$  cm, where  $p_t$  is the transverse momentum in the laboratory frame and  $dr$  and  $dz$  are the radial and axial coordinates of the point of closest approach of the track to the nominal IP, respectively, and the  $z$ -axis is the direction opposite to the positron beam axis;
- the sum of the magnitudes of the momenta of all tracks,  $\Sigma p$ , and the total energy deposit in the ECL are less than 6 GeV/c and 6 GeV, respectively;
- the invariant mass of these four tracks is less than 4.5 GeV/c<sup>2</sup>, and the missing mass squared of the event is greater than 2 GeV<sup>2</sup>/c<sup>4</sup>.

At stage II pairs of oppositely charged tracks without particle identification are used to reconstruct  $K_S^0 \rightarrow \pi^+\pi^-$  decays. To distinguish  $\gamma\gamma \rightarrow K_S^0 K_S^0$  events from other four-track background sources such as  $\gamma\gamma \rightarrow 2(\pi^+\pi^-)$ ,  $\gamma\gamma \rightarrow 2(K^+K^-)$ , and  $\gamma\gamma \rightarrow K^+K^-\pi^+\pi^-$  that have no  $K_S^0$  candidates, two different sets of selections are applied to the  $K_S^0$  candidates with high (low) momentum, i.e. with momentum  $\gtrsim 1.5$  GeV/c (0.5–1.5 GeV/c):  $dr$  is required to be larger than 0.02 (0.03) cm for both charged tracks; the  $\pi^+\pi^-$  vertex is required to be displaced from the IP by a minimum transverse distance of 0.22 (0.08) cm. The mismatch in the  $z$  direction at the  $K_S^0$  vertex point for the  $\pi^+\pi^-$  tracks must be less than 2.4 (1.8) cm; the direction of the pion-pair momentum must also agree with the direction from the IP to the vertex to within 0.03 (0.1) rad. To evaluate the background and calculate efficiencies, we use a Monte Carlo simulation (MC) of the detector response based on GEANT3 [9]. The TREPS code [10] is used for  $\gamma\gamma \rightarrow K_S^0 K_S^0$  event generation and the background  $\gamma\gamma \rightarrow 2(\pi^+\pi^-)$ ,  $\gamma\gamma \rightarrow 2(K^+K^-)$  event generation. From MC simulation, with the described  $K_S^0$  selection above the  $K_S^0$  signal efficiency can reach  $\sim 80\%$  while the background is reduced by a factor of  $10^5$ . Thus the four-track backgrounds can be eliminated efficiently after our event selection. The resolution in the reconstructed  $K_S^0$  mass is 4 MeV/c<sup>2</sup>, and only candidates for which  $|M(\pi^+\pi^-) - m_{K_S^0}| < 13$  MeV/c<sup>2</sup> are selected. Finally, we require that the sum of the transverse momentum vectors of all tracks in the c.m. frame of the  $e^+e^-$  beams,  $|\Sigma \mathbf{p}_t^{ee}|$ , be smaller than 0.1 GeV/c (momentum balance).  $W$  is calculated from the invariant mass of the  $K_S^0 K_S^0$  pair, and  $|\cos\theta^*|$  is obtained from the  $K_S^0$  scattering angle with respect to the incident axis of the electron in the  $\gamma\gamma$  c.m. frame, which approximates the direction of the incoming photon. Fig. 1 shows the  $\pi^+\pi^-$  invariant mass spectra after stage I and stage II selection. After applying the above selections, we find 981  $K_S^0 K_S^0$  candidates in the range 2.4 GeV <  $W$  < 4.0 GeV and  $|\cos\theta^*| < 0.6$ . The  $W$  distribution is shown in Fig. 2. Clear signals for the  $\chi_{c0}$  and  $\chi_{c2}$  resonances are observed.

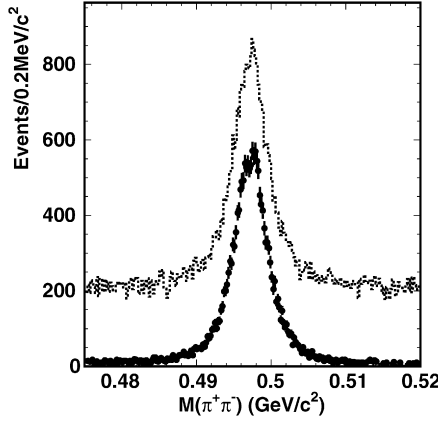


Fig. 1. The  $\pi^+\pi^-$  invariant mass spectrum for  $K_S^0$  candidates after stage I (dotted histogram) and stage II (points with error bars)  $K_S^0$  selection. Here events are selected in the range  $W = 2.3\text{--}4.5$  GeV and  $|\Sigma \mathbf{p}_i^{ee}| < 0.25$  GeV/c, where  $W$  and  $|\Sigma \mathbf{p}_i^{ee}|$  are calculated by assuming all tracks are charged pions.

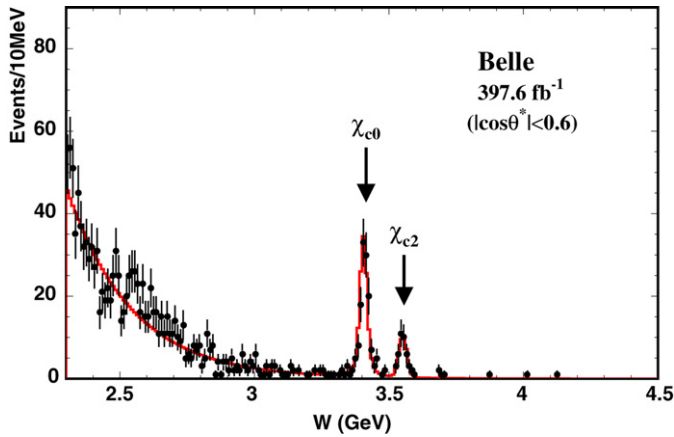


Fig. 2.  $K_S^0 K_S^0$  mass spectrum before background subtraction. The curves show the fit result described later in the section on  $\chi_{cJ}$  resonances.

### 3. Background subtraction

The background contamination from events where additional particles accompany the two detected  $K_S^0$  mesons—so-called non-exclusive backgrounds—should be also estimated. Because of the available phase space, such events are expected to have a  $|\Sigma \mathbf{p}_i^{ee}|$  distribution that is close to zero at  $|\Sigma \mathbf{p}_i^{ee}| = 0$  and increases with  $|\Sigma \mathbf{p}_i^{ee}|$ . This feature is verified in the  $\gamma\gamma \rightarrow K_S^0 K_S^0 \pi^0$  (which is the dominant background) MC and data sample, where the MC sample is generated by using GGLU code [11]. We assume that the  $|\Sigma \mathbf{p}_i^{ee}|$  distribution of the non-exclusive background can be parameterized by

$$f(x) = \begin{cases} cx, & x \leq 0.05 \text{ (GeV/c)}, \\ ax + b, & x \geq 0.05 \text{ (GeV/c)}, \end{cases}$$

constrained by  $0.05c = 0.05a + b$ . We fit the function  $f(x)$  to the difference between data and signal MC distributions which is normalized to the data below 0.03 GeV/c where the background contribution is negligibly small (Fig. 3). Using the data sample with  $|\Sigma \mathbf{p}_i^{ee}| = 0.5\text{--}1.0$  GeV/c we verify that there is no  $\theta^*$  dependence of the shape. Using the fit results, the estimated background, which is  $4.1 \pm 0.1\%$ ,  $3.6 \pm 0.2\%$ , and

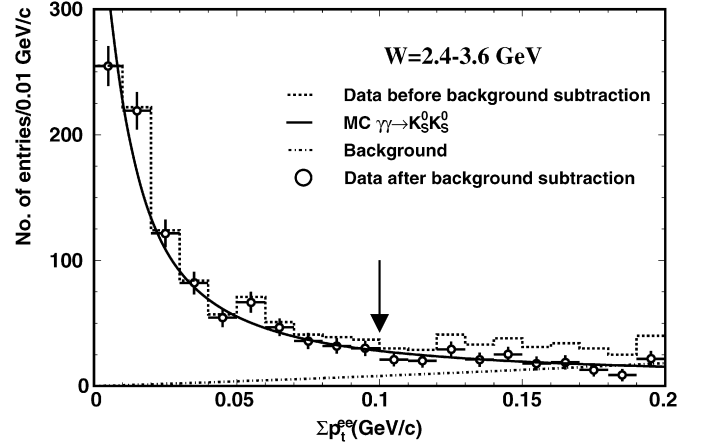


Fig. 3.  $|\Sigma \mathbf{p}_i^{ee}|$  distribution for  $K_S^0 K_S^0$  candidates. The dotted histogram and points with error bars indicate the distribution of events before and after background subtraction, respectively. The dot-dashed line is the background distribution, which is obtained from the fit to the difference between MC and data. The solid curve shows the signal MC distribution, which is normalized to the number of signal candidates in the three leftmost bins. The arrow indicates the upper boundary of the  $|\Sigma \mathbf{p}_i^{ee}|$  requirement for the signal.

$2.6 \pm 0.3\%$  for  $W = 2.4\text{--}2.6$  GeV,  $2.6\text{--}2.8$  GeV,  $2.8\text{--}3.3$  GeV, respectively, is subtracted in each  $W$  bin (the errors are statistical only). For  $W = 3.6\text{--}4.0$  GeV, the background is set to zero since the data sample is too small to apply the procedures described above.

Finally, 952 signal events remain in the signal region  $|\Sigma \mathbf{p}_i^{ee}| < 0.1$  GeV/c after background subtraction.

### 4. Cross sections of the process $\gamma\gamma \rightarrow K_S^0 K_S^0$ for $2.4 \text{ GeV} < W < 4.0 \text{ GeV}$

The differential cross section for two-photon production of the final state  $X$  in electron–positron collisions is given by

$$\begin{aligned} & \frac{d\sigma}{d|\cos\theta^*|}(W, |\cos\theta^*|; \gamma\gamma \rightarrow X) \\ &= \frac{\Delta N(W, |\cos\theta^*|; e^+e^- \rightarrow e^+e^- X)}{\mathcal{L}_{\gamma\gamma}(W) \Delta W \Delta|\cos\theta^*| \epsilon(W, |\cos\theta^*|) \mathcal{L}_{\text{int}}}, \end{aligned} \quad (3)$$

where  $\Delta N$  and  $\epsilon$  denote the number of signal events after background subtraction and the product of detection and trigger efficiencies, respectively. The integrated luminosity of this experiment,  $\mathcal{L}_{\text{int}}$ , is  $397.6 \text{ fb}^{-1}$  and is determined with a systematic uncertainty of 1.4%. The luminosity function  $\mathcal{L}_{\gamma\gamma}$ , as a function of  $W$ , is defined by

$$\mathcal{L}_{\gamma\gamma}(W) = \frac{\frac{d\sigma}{dW}(W; e^+e^- \rightarrow e^+e^- X)}{\sigma(W; \gamma\gamma \rightarrow X)}. \quad (4)$$

The efficiencies  $\epsilon(W, |\cos\theta^*|)$  are obtained from MC using the TREPS code [10] for  $\gamma\gamma \rightarrow K_S^0 K_S^0$  event generation. The TREPS code is also used for the luminosity function determination. Trigger efficiencies are determined from the trigger simulator. The typical values of the detection and trigger efficiency are 5–19% and 90–95%, respectively, and grow with increasing  $W$  and decreasing  $|\cos\theta^*|$ . Differential cross sections normalized to the cross section integrated over the range

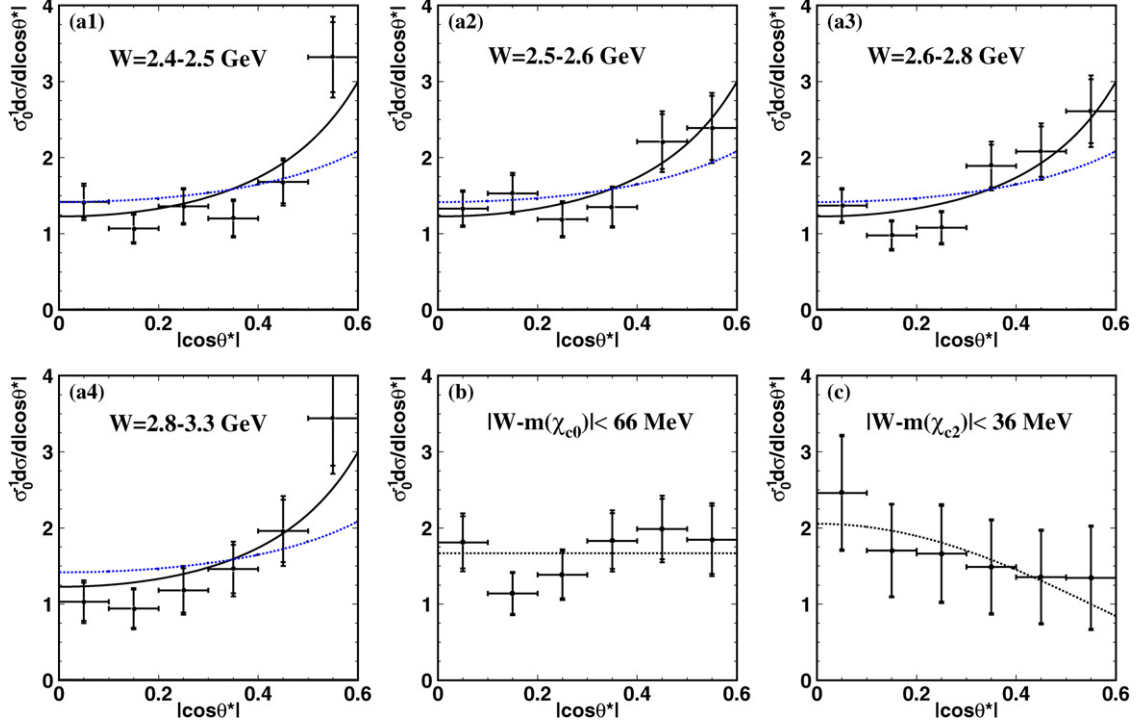


Fig. 4. (a1)–(a4) The angular distribution of the cross section,  $\sigma_0^{-1} d\sigma/d|\cos\theta^*|$ , in different  $W$  ranges. The solid curves are  $1.227 \sin^{-4}\theta^*$ , which is the prediction of DKV. The dotted curves are the prediction of BC. (b) The angular distribution in the  $\chi_{c0}$  region; the dotted curve shows a flat distribution ( $J=0$ ). (c) The angular distribution in the  $\chi_{c2}$  region; the dotted curve shows the helicity 2 distribution ( $\propto \sin^4\theta^*$ ). The errors indicated by short ticks are statistical only.

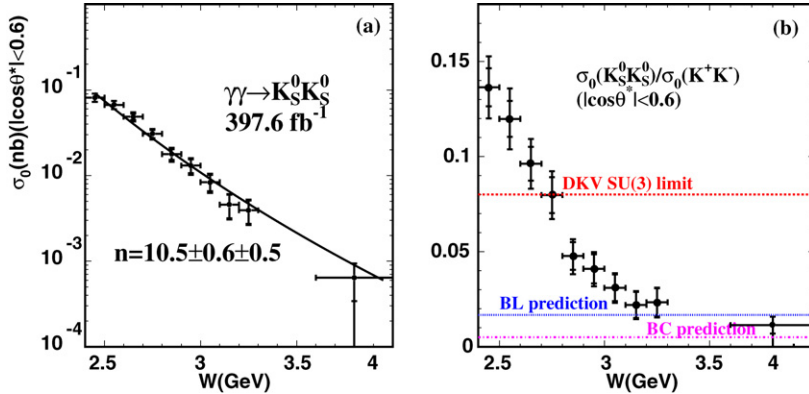


Fig. 5. (a) Total cross sections for  $\gamma\gamma \rightarrow K_S^0 K_S^0$  in the c.m. angular region  $|\cos\theta^*| < 0.6$ . Here  $n$  is the  $W$ -dependence ( $\propto W^{-n}$ ). (b) The ratio  $\sigma_0(K_S^0 K_S^0)/\sigma_0(K^+ K^-)$  versus  $W$  in  $|\cos\theta^*| < 0.6$ , where the  $K^+ K^-$  data are taken from the Belle measurement [4]. The dotted line is the DKV prediction with the flavor symmetry assumption; the dashed and dashed-dotted lines are the BL and BC predictions, respectively. The two sets of error bars show the statistical and combined statistical + systematic errors, respectively.

$|\cos\theta^*| < 0.6$  ( $\sigma_0$ ) in different  $W$  bins are shown in Fig. 4(a). The angular distributions are consistent with both BC and DKV predictions up to  $|\cos\theta^*| = 0.5$ .

The angular distributions,  $\sigma_0^{-1} d\sigma/d|\cos(\theta^*)|$ , in the  $\chi_{c0}$  and  $\chi_{c2}$  regions ( $|W - m(\chi_{c0})| < 66 \text{ MeV}/c^2$ ,  $|W - m(\chi_{c2})| < 36 \text{ MeV}/c^2$ ) shown in Figs. 4(b), (c) are in good agreement with those expected for the decays of the spin zero and two particles. The total cross section  $\sigma_0$  as a function of  $W$  is shown in Fig. 5(a) and listed in Table 1. The values of the total cross section for the range,  $W = 3.3\text{--}3.6 \text{ GeV}$ , where the contribution from charmonium states is large, are omitted.

## 5. Systematic errors

The dominant systematic errors are summarized in Table 2. We assign 4% to the uncertainty from trigger, which is determined by comparing the trigger efficiencies in the data sample and trigger simulation. The uncertainty of  $K_S^0$  reconstruction efficiency is estimated by comparing the ratio of the number of  $\gamma\gamma \rightarrow K_S^0 K_S^0$  events with both  $K_S^0$  mesons satisfying the selection requirements and that with only one  $K_S^0$  satisfying the requirements in data and MC samples. We take the efficiency difference between the data and MC  $\gamma\gamma \rightarrow K_S^0 K_S^0$  sample,

Table 1

Signal yields ( $N_{\text{ev}}$ ) and total cross sections ( $\sigma_0$ ) for the process  $\gamma\gamma \rightarrow K_S^0 K_S^0$  in the angular range  $|\cos\theta^*| < 0.6$ . The first and second errors are statistical and systematic, respectively

$W$ (GeV)	$N_{\text{ev}}$	$\sigma_0$ , nb
2.4–2.5	$226.3 \pm 15.4$	$0.0816 \pm 0.0056 \pm 0.0070$
2.5–2.6	$195.6 \pm 14.3$	$0.0671 \pm 0.0049 \pm 0.0057$
2.6–2.7	$137.9 \pm 12.0$	$0.0488 \pm 0.0042 \pm 0.0042$
2.7–2.8	$81.9 \pm 9.2$	$0.0307 \pm 0.0034 \pm 0.0027$
2.8–2.9	$46.8 \pm 6.9$	$0.0178 \pm 0.0026^{+0.0016}_{-0.0021}$
2.9–3.0	$31.1 \pm 5.7$	$0.0131 \pm 0.0024^{+0.0012}_{-0.0016}$
3.0–3.1	$21.4 \pm 4.7$	$0.0084 \pm 0.0018^{+0.0008}_{-0.0010}$
3.1–3.2	$10.7 \pm 3.3$	$0.0046 \pm 0.0014^{+0.0004}_{-0.0006}$
3.2–3.3	$10.7 \pm 3.3$	$0.0039 \pm 0.0012^{+0.0004}_{-0.0005}$
3.6–4.0	$5.0 \pm 2.2$	$0.0006 \pm 0.0003^{+0.0001}_{-0.0006}$ ( $< 0.0013$ at 90% CL)

Table 2

Summary of systematic errors

Source	Error, %
Trigger efficiency	4
Luminosity function	3.4–5.0
Background (for non-resonant analysis)	2.0–8.4
$K_S^0$ reconstruction (per $K_S^0$ )	4.4
Integrated luminosity	1.4
Total	8.5–12.1

which is 4.4% for one  $K_S^0$ . The uncertainties in the background subtraction are estimated by fitting the background shape in the  $|\Sigma \mathbf{p}_i^{ee}|$  distributions using second-order polynomial functions and comparing the background fractions obtained to those described above. The differences between the two calculations are taken as the corresponding systematic error in each energy range and are 2.0%, 2.0%, and  $^{+8.4}_{-2.6}\%$  for  $W = 2.4$ –2.6 GeV, 2.6–2.8 GeV, 2.8–3.3 GeV, respectively. For  $W = 3.6$ –4.0 GeV, we conservatively assign the number of observed events as the systematic error in the background. The 3.4–5.0% systematic error for the luminosity function in the range  $W = 2.4$ –4.0 GeV in Ref. [10] is determined from comparison of the kinematic distributions for the two-photon system in events generated with TREPS to those from a QED calculation that includes all order  $\alpha^4$  diagrams [12]. The total  $W$ -dependent systematic error is (8.5–12.1)%.

## 6. Discussion

The leading term in QCD calculations [1,2] predicts a  $\sim W^{-6}$ -dependence of the cross sections  $d\sigma/d\cos\theta^*$  ( $\gamma\gamma \rightarrow M\bar{M}$ ). However, the fit to the data in the range  $W = 2.4$ –4.0 GeV gives a  $W$ -dependence ( $\sigma_0 \propto W^{-n}$ ) of  $n = 10.5 \pm 0.6 \pm 0.5$ , where the first error is statistical and the second is systematic. We conservatively estimate the systematic error on  $n$  by artificially deforming the measured cross section values assuming that the systematic errors are strongly correlated point-to-point, as in Ref. [4]: we shift the  $\sigma_0$  values at the two end bins by  $\pm 1.5$  and  $\mp 1.5$  times the systematic error, respec-

tively, whereas each intermediate point is moved so that its shift follows a linear function of  $W$  times its systematic error. The average of the observed deviations in  $n$  from its original value is taken as a final systematic error. The value of  $n$  indicates that, unlike  $\gamma\gamma \rightarrow \pi^+\pi^-$  and  $\gamma\gamma \rightarrow K^+K^-$  [4], the current values of  $W$  are not yet large enough to neglect power corrections in  $\gamma\gamma \rightarrow K_S^0 K_S^0$ , which are not taken into account in the BL and BC predictions.

The ratio  $\sigma_0(K_S^0 K_S^0)/\sigma_0(K^+ K^-)$  shown in Fig. 5(b) decreases from  $\sim 0.13$  to  $\sim 0.01$  with increasing  $W$ . This energy dependence is inconsistent with the DKV prediction that the ratio should be  $\approx 2/25$  in the SU(3) symmetry limit. Furthermore, it is difficult to explain the experimental result with the handbag model even if the effect of SU(3)-symmetry breaking is taken into account [6,13]. This indicates that the handbag model needs significant corrections.

Since the experimental values of the ratio  $\sigma_0(K_S^0 K_S^0)/\sigma_0(K^+ K^-)$  approach the BL and BC predictions at the highest measured energies  $W \approx 4$  GeV, the leading term QCD calculations [1,2] may become applicable for  $\sigma(K_S^0 K_S^0)$  at not much larger values of  $W$ .

## 7. The two-photon decay width of $\chi_{cJ}$ resonances

Measurements of  $\gamma\gamma \rightarrow K_S^0 K_S^0$  can also provide more precise results [14] for the two-photon decay widths and branching fractions of the charmonium states since the continuum background is strongly suppressed. By fitting the continuum  $M(K_S^0 K_S^0)$  distribution to an exponential distribution and parameterizing the charmonium peaks with a Breit–Wigner function for the  $\chi_{c0}$  and Gaussian function for the narrow  $\chi_{c2}$  with the masses and widths floating,  $134 \pm 12 \chi_{c0}$  and  $38 \pm 7 \chi_{c2}$  events are observed. The masses and widths obtained from the fit taking into account the detector resolution are consistent with the PDG values. The  $\chi_{c0}$  ( $\chi_{c2}$ ) statistical significance is  $22.7\sigma$  ( $11.2\sigma$ ), where  $\sigma$  is a standard deviation. The statistical significance of the signals is obtained from the  $\sqrt{-2\ln(L_0/L_{\text{max}})}$  values, where  $L_{0(\text{max})}$  is the likelihood without (with) the signal contribution, with the joint estimation of the three parameters (mass, width, and yield are determined simultaneously). The two-photon decay width of the  $\chi_{c0}$  or  $\chi_{c2}$  can be obtained using the formula

$$\Gamma_{\gamma\gamma}(\chi_{cJ}) \times \mathcal{B}(\chi_{cJ} \rightarrow K_S^0 K_S^0) = \frac{Y m^2}{4(2J+1)\pi^2 \mathcal{L}_{\gamma\gamma}(m) \epsilon \mathcal{B}^2(K_S^0 \rightarrow \pi^+\pi^-) \mathcal{L}_{\text{int}}}, \quad (5)$$

where  $Y$  and  $m$  are the yield and mass of the  $\chi_{cJ}$  charmonium state, respectively. The quantity  $\epsilon$  denotes the product of the detector efficiency, trigger efficiency, and angular acceptance for the resonant decays. In addition to the sources of systematic errors listed in Table 2, the errors in the yield are 2.3% and 2.4% for the  $\chi_{c0}$  and  $\chi_{c2}$ , respectively. For  $\chi_{c2}$  events we assume a pure helicity 2 state in MC generation following the previous measurement [15] and theoretical expectations [16,17]. The directly measured values of the product  $\Gamma_{\gamma\gamma}(\chi_{cJ}) \mathcal{B}(\chi_{cJ} \rightarrow K_S^0 K_S^0)$  are  $7.00 \pm 0.65 \pm 0.6$  eV for the  $\chi_{c0}$

Table 3

The products of the two-photon width and the branching fraction, ratios of the branching fractions, and two-photon widths for the  $\chi_{c0}$  and  $\chi_{c2}$ . The notation *br.* indicates the systematic uncertainty from the branching fraction of  $\chi_{cJ} \rightarrow K_S^0 K_S^0$

Resonance	$\chi_{c0}$	$\chi_{c2}$
$\Gamma_{\gamma\gamma} \mathcal{B}(K_S^0 K_S^0)$ , eV	$7.00 \pm 0.65 \pm 0.71$	$0.31 \pm 0.05 \pm 0.03$
$\mathcal{B}(K_S^0 K_S^0)/\mathcal{B}(K^+ K^-)$	$0.49 \pm 0.07 \pm 0.08$	$0.70 \pm 0.21 \pm 0.12$
$\mathcal{B}(K_S^0 K_S^0)/\mathcal{B}(\pi^+ \pi^-)$	$0.46 \pm 0.08 \pm 0.07$	$0.40 \pm 0.10 \pm 0.06$
$\Gamma_{\gamma\gamma}$ , keV	$2.50 \pm 0.23 \pm 0.23 \pm 0.62(br.)$	$0.46 \pm 0.08 \pm 0.04 \pm 0.08(br.)$

and  $0.31 \pm 0.05 \pm 0.03$  eV for the  $\chi_{c2}$ . Using the results of our previous measurement of  $K^+ K^-$  and  $\pi^+ \pi^-$  production in  $\gamma\gamma$  collisions [4], we determine the ratios  $\mathcal{B}(K_S^0 K_S^0)/\mathcal{B}(K^+ K^-)$  and  $\mathcal{B}(K_S^0 K_S^0)/\mathcal{B}(\pi^+ \pi^-)$  for the  $\chi_{c0}$  and  $\chi_{c2}$ , in which some common systematic errors cancel. Here  $\mathcal{B}(\pi^+ \pi^-)$ ,  $\mathcal{B}(K^+ K^-)$  and  $\mathcal{B}(K_S^0 K_S^0)$  are the branching fractions for the  $\chi_{cJ}$  decay to the corresponding final state. Using the world-average values of the branching fractions  $\mathcal{B}(\chi_{c0} \rightarrow K_S^0 K_S^0) = (2.8 \pm 0.7) \times 10^{-3}$  and  $\mathcal{B}(\chi_{c2} \rightarrow K_S^0 K_S^0) = (6.7 \pm 1.1) \times 10^{-4}$  [14], from the products of the widths and branching fractions given above we can extract the values of the two-photon width that are shown in Table 3. The notation *br.* indicates the systematic uncertainty from the branching fraction of  $\chi_{cJ} \rightarrow K_S^0 K_S^0$ . It can be seen that for both the  $\chi_{c0}$  and  $\chi_{c2}$  the value of  $\mathcal{B}(K_S^0 K_S^0)/\mathcal{B}(K^+ K^-)$  is compatible with 0.5 as expected from isospin symmetry. The values of the two-photon widths of the  $\chi_{c0(2)}$  charmonia are consistent with those obtained from their total width and the branching fractions for decay to two photons in Ref. [14].

## 8. Conclusion

Using a  $397.6 \text{ fb}^{-1}$  data sample accumulated with the Belle detector at KEKB, the cross sections of the process  $\gamma\gamma \rightarrow K_S^0 K_S^0$  have been measured for the first time in the  $W$  range from 2.4 to 4.0 GeV with  $|\cos\theta^*| < 0.6$ . The overall  $W$ -dependent systematic uncertainty is 8.5–12.1%. The measured  $W$ -dependence ( $\sigma_0 \propto W^{-n}$ ) of  $\gamma\gamma \rightarrow K_S^0 K_S^0$  is  $n = 10.5 \pm 0.6 \pm 0.5$  from a fit to the data with  $W = 2.4\text{--}4.0$  GeV, indicating that, unlike  $\gamma\gamma \rightarrow \pi^+ \pi^-$  and  $\gamma\gamma \rightarrow K^+ K^-$ , the  $W$  values up to 3.3 GeV are not sufficiently large to apply the leading term BL and BC predictions to  $\gamma\gamma \rightarrow K_S^0 K_S^0$ . The angular distribution in the range  $|\cos\theta^*| < 0.5$  is consistent with both BC and DKV. The ratio  $\sigma_0(\gamma\gamma \rightarrow K_S^0 K_S^0)/\sigma_0(\gamma\gamma \rightarrow K^+ K^-)$  decreases rapidly from  $\sim 0.13$  to  $\sim 0.01$  with increasing  $W$  in contrast to the expectation from the DKV model. Since the measured values of the cross section ratio approach the BL and BC predictions in the highest energy bin, 3.6–4.0 GeV, this may indicate that the leading term QCD calculations for  $\sigma(\gamma\gamma \rightarrow K_S^0 K_S^0)$  are already applicable at  $W$  values larger than  $\sim 4$  GeV. In addition, the products of the two-photon decay width and branching ratio to  $K_S^0 K_S^0$  for the  $\chi_{c0}$  and  $\chi_{c2}$  are found to be  $7.00 \pm 0.65 \pm 0.71$  eV and  $0.31 \pm 0.05 \pm 0.03$  eV.

## Acknowledgements

We are grateful to S.J. Brodsky, V.L. Chernyak, M. Diehl, G. Duplančić, P. Kroll, H.-N. Li, K. Odagiri, and R.-C. Verma

for fruitful discussions. We thank the KEKB group for the excellent operation of the accelerator, the KEK cryogenics group for the efficient operation of the solenoid, and the KEK computer group and the National Institute of Informatics for valuable computing and Super-SINET network support. We acknowledge support from the Ministry of Education, Culture, Sports, Science, and Technology of Japan and the Japan Society for the Promotion of Science; the Australian Research Council and the Australian Department of Education, Science and Training; the National Science Foundation of China and the Knowledge Innovation Program of the Chinese Academy of Sciences under contract No. 10575109 and IHEP-U-503; the Department of Science and Technology of India; the BK21 program of the Ministry of Education of Korea, the CHEP SRC program and Basic Research program (grant No. R01-2005-000-10089-0) of the Korea Science and Engineering Foundation, and the Pure Basic Research Group program of the Korea Research Foundation; the Polish State Committee for Scientific Research; the Ministry of Education and Science of the Russian Federation and the Russian Federal Agency for Atomic Energy; the Slovenian Research Agency; the Swiss National Science Foundation; the National Science Council (under Grant No. NSC 94-2112-M-008-027) and the Ministry of Education of Taiwan; and the US Department of Energy.

## References

- [1] S.J. Brodsky, G.P. Lepage, Phys. Rev. D 24 (1981) 1808.
- [2] M. Benayoun, V.L. Chernyak, Nucl. Phys. B 329 (1990) 209.
- [3] A. Heister, et al., ALEPH Collaboration, Phys. Lett. B 569 (2003) 140.
- [4] H. Nakazawa, et al., Belle Collaboration, Phys. Lett. B 615 (2005) 39.
- [5] M. Diehl, P. Kroll, C. Vogt, Phys. Lett. B 532 (2002) 99.
- [6] V.L. Chernyak, Phys. Lett. B 640 (2006) 246.
- [7] A. Abashian, et al., Belle Collaboration, Nucl. Instrum. Methods A 479 (2002) 117.
- [8] S. Kurokawa, E. Kikutani, Nucl. Instrum. Methods A 499 (2003) 1, and other papers included in this volume.
- [9] The detector response is simulated with GEANT, R. Brun, et al., GEANT 3.21, CERN Report DD/EE/84-1, 1984.
- [10] S. Uehara, KEK Report 96-11, July 1996.
- [11] egpc v207, L3 program library, 1999, converted to the Belle configuration by S. Hou, 2000.
- [12] F.A. Berends, P.H. Daverveldt, R. Kleiss, Nucl. Phys. B 253 (1985) 441.
- [13] M. Diehl, Wide-angle processes, Talk at Int. Workshop ‘‘GPD2006’’, Trento, Italy, 6 June 2006.
- [14] W.-M. Yao, et al., Particle Data Group, J. Phys. G 33 (2006) 1.
- [15] K. Abe, et al., Belle Collaboration, Phys. Lett. B 540 (2002) 33.
- [16] M. Poppe, Int. J. Mod. Phys. A 1 (1986) 545.
- [17] H. Krasemann, J.A.M. Vermaseren, Nucl. Phys. B 184 (1981) 269.